Acta Mechanica Slovaca **27 (3): 42 - 52,** September **2023**
https://doi.org/10.21496/ams.2023.032

Acta Mechanica Slovaca
ISSN 1335-2393
www.actamechanica.sk

Analysis of the Tribothermal and Mechanical Behavior of Copper-Steel and Brass-Steel Sliding Couples

Boubechou Choubeila [1*], Bouchoucha Ali [2], Bouzaouit Azeddine [1]

[1] Faculty of Technology, Department of Mechanical Engineering, University of 20 August 1955, Skikda 21000, Algeria
[2] Laboratoire de Mécanique, Faculté des Sciences de la Technologie, Département de Mécanique Engineering, Université Constantine1, 25000, Algeria

Abstract: This article deals with a comparative study of the thermomechanical behavior of copper-steel and brass-steel tribological couples, as a function of functional parameters: contact mode, dynamic torsor, contact kinematics and the materials making up the tribosystem. For this purpose, friction and wear tests were carried out using a pin-disc tribometer, in an atmospheric environment. This consists of a copper or brass pin rubbing dry against a rotating steel disc. A Comsol Multiphysics numerical code was used to evaluate contact temperature, mechanical stresses and deformations at the interface of the pairs. The results obtained show that the above-mentioned parameters have a significant influence on the tribomechanical and thermal behavior of the two couples. Indeed, the dissipation of heat by sliding modifies the physicochemical and mechanical properties of the materials, and promotes the oxidation process. In addition to the formation of oxides, the mutual material transfer mechanism plays a key role in the friction and wear of the couples. The discussion of the results is based on macroscopic and microscopic observations of worn surfaces and the interfacial phenomena resulting from sliding.

Keywords: Copper; Brass; Steel; Interface; Friction; Wear; Oxidation; Contact Temperature; Stresses; Deformations.

1. Introduction

Copper's face-centered cubic lattice is sensitive to adhesion, and its alloys are materials with a wide range of applications in the industrial sector. Indeed, copper itself is characterized by good electrical and thermal conductivity, and above-average corrosion resistance. In mechanical engineering, pure copper cannot generally be used (in certain mechanical applications) due to its mechanical properties. It is therefore combined with other elements (e.g. zinc, tin, lead) in concentrations ranging from 5 to 45% to produce alloys with good mechanical and tribological properties. This is why these alloys are used as antifriction materials in many industrial applications [1-2].

Generally speaking, in a dynamic contact, friction is characterized by an overall coefficient of friction; from a physical point of view, taking into account operating parameters and material properties [3].

These different mechanisms vary according to the nature and properties of the materials involved, as well as the conditions under which contact takes place - environment, temperature, load and speed.

We also know that friction is an energy dissipation mechanism that can take different forms:

*** Corresponding author:** Boubechou Choubeila, ***E-mail address:*** *choubeila_boubechou@yahoo.fr*

– mechanical dissipation through deformation, plasticization, epidermal creep, elastic hysteresis;
– wear and tear, debris stripping;
– thermal dissipation, contact heating, sparking;
– physicochemical phenomena, oxidation, corrosion, chemical reactions, phase changes, diffusion of elements [4].

In addition, to understand the behavior of the interface, from the point of view of heat and matter transfer; by varying the dynamic and kinematic parameters and the nature of the materials in sliding contact; a tribothermal study is necessary, in most mechanical systems.

The aim of this work is to understand the mechanisms of friction and wear, and the physicochemical phenomena resulting from friction. In addition, a comparison of the tribological and thermomechanical behavior of the two couples will be carried out, with the aim of optimizing their operating conditions and thus their service life.

2. Materials and experimental procedure

The experimental device is a pin-on-disc tribometer. Tests are carried out in an ambient air. The pin (copper and brass) and disc are made of steel (Fig.1) and their characteristics are presented in tables 1 and 2. The disc is driven in a rotational movement of constant velocity with diameter of 50 mm and 12 mm of thickness. It has a lame hole in the center.

The normal load is vertically applied with a weight P. The pin has a cylindrical shape of length 20mm and a diameter of 8mm; has a flat allows to fix it in a hole with a screw on an arm load of aluminum. Friction coefficient m is deduced from

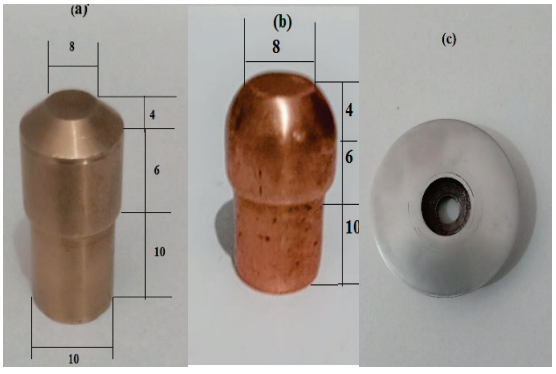

Figure 1: Shape of pins: (a) Brass pin. (b) Copper pin. (c) Steel disc.

measurement of the tangential force F induced on the arm by the rotating wheel through the pin (μ=F/P) (Fig.2). The wear W is determined by weighing the specimen before and after each test using a balance with a precision of ±0.1mg. To ensure the same experimental conditions for each test, the disc is polished mechanically with a 1200 grain paper. The duration of each test is 30 minutes.

The diameter of the pin is constant, unless we take into account variations due to expansion, which depend on the temperature rise at the interface. These variations in pin diameter therefore depend on the thermal properties of the materials. If we neglect these expansions, during operation of the two couples, the apparent diameters of the pins are identical. However, as the pins wear, their length decreases due to the removal of material. This decrease depends, above all, on the tribological conditions, the properties of the facing materials, and the operating factors of the couples.

Table 1: Chemical composition of couple materials.

Composition / Materials	Cu	Zn	Pb	Fe	Ni	Mn	S	Cr	Mo
Cu	99.99	-	-						
CuZn40Pb3	57	40	3						
41CrMo4				96.86	0.16	0.94	0.01	1.05	0.21

Table 2: Mechanical and physical properties of steel, copper and brass.

Materials	E [N/mm^2]	Rm [N/mm^2]	A%	HB	ρ [kg/m^3]	λ [W/m°C]	γ [$\mu\Omega$.m]	C_p [J/kg°C]
Cu	12600	210	50	250	$8.5.10^3$	121	0.062	377
CuZn40Pb3	96000	460	15	120	$8.940.10^3$	384	0.017	380
41CrMo4	207000	min 650	min 12	270-330	$7.8.10^3$	44	0.24	480

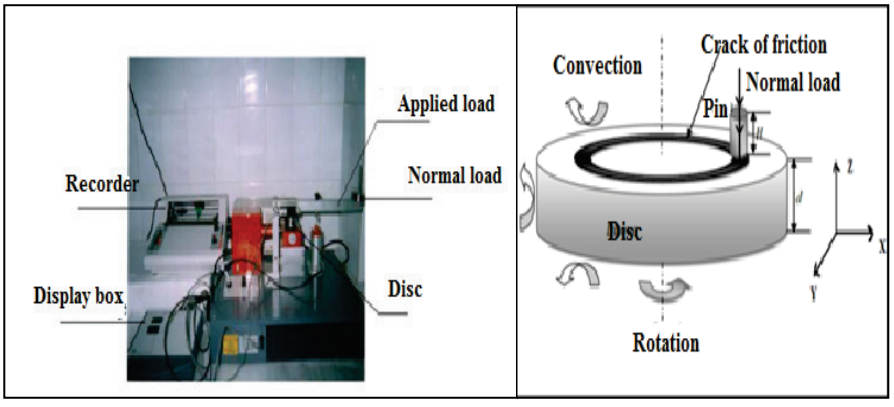

Figure 2: (a) Tribometer apparatus. (b) Contact pin on disc.

3. Mechanical stresses and strains

The materials are isotropic.

3.1. Boundary conditions

It is assumed that:

- *the contact between the pin and the disc is considered perfect.*
- *the load is applied to the center of the pin at its upper face.*

3.2. Stress tensor

The state of stress at a point A is characterized by the stress tensor. It is a symmetrical second order tensor. In an orthonormal basis, it is represented by the stress matrix, denoted σij and is written:

$$\sigma_{ij} = \begin{bmatrix} \sigma_{11} & \sigma_{12} & \sigma_{13} \\ \sigma_{21} & \sigma_{22} & \sigma_{23} \\ \sigma_{31} & \sigma_{32} & \sigma_{33} \end{bmatrix} \quad (1)$$

The mechanical boundary conditions correspond either to a displacement, or to a normal or tangential stress imposed on different zones. There are three degrees of freedom in displacement, so there are three equations to solve simultaneously to determine the boundary conditions. The three stresses imposed on the top surface of normal mass are σ_{XX}, σ_{YY} and σ_{ZZ}, called normal stresses or pressures and σ_{XY} and σ_{XZ} tangential stresses (Fig.3).

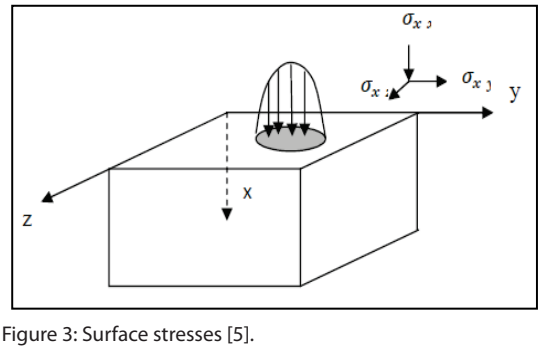

Figure 3: Surface stresses [5].

3.3. Thermal dissipation

3.3.1. Physical equations and boundary conditions of the transient thermal problem

We define the energy equation in Cartesian coordinates as follows:

$$\rho C_p \left(\frac{dT}{dt} \right) = \nabla (\lambda \nabla T) + S + \mu\phi \quad (2)$$

The following assumptions are considered:

- *the viscous dissipation and the compressibility effect are negligible.*

Equation (2) becomes:

$$\rho C_p \left(\frac{\partial T}{\partial t} + V \nabla T \right) = \lambda \nabla^2 T \quad (3)$$

Solving our problem amounts to solving the heat equation in cartesian coordinates with the presence of a surface heat source. It takes the following form [6]:

» *for the disc:*

$$\lambda_d \Delta T_d = \rho_d C_{pd} \left(\frac{\partial T}{\partial t} + V \nabla T_d \right) \quad (4)$$

» *for the pin:*

$$\lambda_p \Delta T_p = \rho_p C_{pp} \left(\frac{\partial T_p}{\partial t} \right) \quad (5)$$

3.3.2. In steady state

$$\frac{\partial T}{\partial t} = 0 \quad (6)$$

The equation that governs the heat transfer in the disc is:

$$\lambda_d \Delta T_d = \rho_d C_{pd} V \nabla T_d \quad (7)$$

and in the pin:

$$\lambda_p \Delta T_p = 0 \quad (8)$$

The boundary conditions are specified as follows:

At the contact, we have a heat flow generated by friction between the pin and the disc, it is noted by qt. Outside the contact, we have convection, it is characterized by the heat exchange coefficient hair assumed constant.

4. Results

4.1. Friction and wear behavior

4.1.1. Variation of the friction coefficient as a function of time

Figure4 shows the evolution of the friction coefficient as a function of time. On this curve we can distinguish two different zones:

– *Area I: transitional running-in or adaptation phase, necessary for the evacuation of particles formed when the two counter-faces come into contact; where μ evolves progressively for brass is (t=1-5min), during which the coefficient of friction fluctuates between two extreme values (0.18-0.28), but for copper is (t=1-15min), this coefficient fluctuates between (0.26-0.45).*

– *Area II: characterizes the stationary regime, in which the state of equilibrium is established, by stability of operating conditions at the interface. The coefficient of friction stabilizes after the fifth minute (μ=0.2) for brass and the fifteenth minute for copper (μ=0.55).*

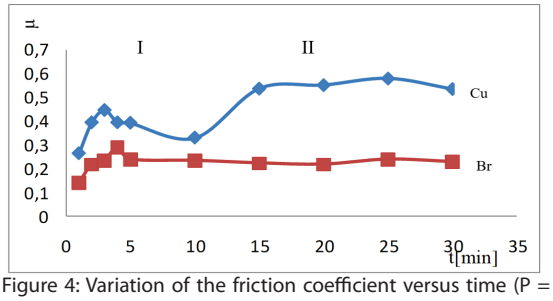

Figure 4: Variation of the friction coefficient versus time (P = 20N and V = 0.5m/s).

4.1.2. Variation of the friction coefficient with the normal load

Figure5 shows the evolution of the friction coefficient with the normal load P, for the couple brass-steel and copper-steel. Two phases can be observed:

– *phase I: the friction coefficient decreases progressively at relatively low loads.*

– *phase II: the friction coefficient stabilizes around μ=0.22 for brass and μ=0.62 for copper. The difference Δμ between the two couples is 0.40.*

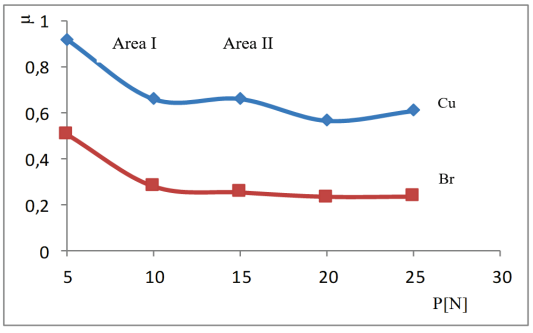

Figure 5: Variation of the friction coefficient versus the load (V=0.5m/s).

4.1.3. Variation of the friction coefficient with the sliding speed

The curves in Figure 6 show that the coefficient of friction is more or less stable for brass and copper at sliding speeds of (0.1m/s to 0.5m/s). It is generally noted that the increase in the sliding speed does not have a significant influence on the coefficient of friction except for the speed 5m/s.

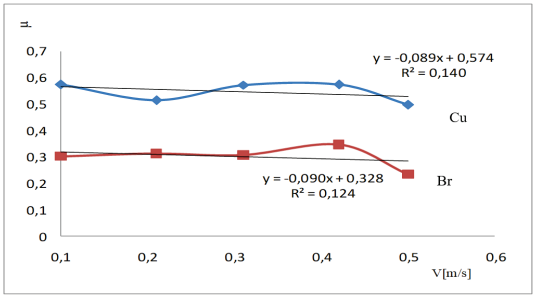

Figure 6: Variation of the friction coefficient versus the speed (P = 20N).

4.1.4. Variation of the wear with the sliding speed

Sliding speed is an essential parameter which has a significant effect on the wear of the tribological pairs studied (brass-steel and copper-steel). Indeed, the curves in Figure7 show the following:

– *for copper-steel: at low speeds, the low mass loss of the pin leads to considerable uncertainties in the value of W, particularly for speeds below 0.2m/s (W=0.00283 g). Above 0.2m/s, wear is quasi-static (W=0.03319 g).*

– *For brass-steel: wear varies between values of 0.075341g and 0.14182g, and the increase in wear is greater for this pair than for the copper-steel couple, the average deviation of the material loss for the same operating conditions is Δm=0.10863g.*

4.1.5. Variation of wear with normal load

Figure8 shows the evolution of wear as a function of the normal load applied. It can be seen that the variation in wear is an increasing linear function with

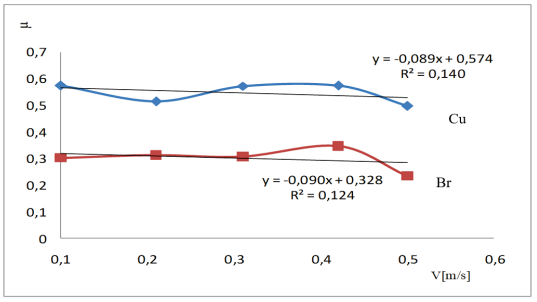

Figure 7: Variation of wear versus sliding speed (P = 20N).

normal load, ranging from 0.06g to 0.15g for loads of 5N to 25N for the brass/steel pair. However, it is very slight for the copper/steel couple from 0.02g to 0.04g.

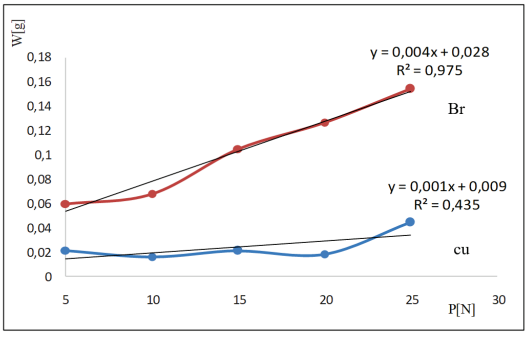

Figure 8: Wear variation versus normal load (V = 0.5 m/s).

4.2. Thermal behavior

4.2.1. Temperature versus contact surface

Figure9 shows the steady state temperature distribution at the contact surface of the two sliding couples for a load of 20N and a speed of 0.5m/s. It can be seen that the closer we get to the contact area at the level of the pin-disc interface, the temperature increases to a maximum value of 393.267K for the copper-steel couple and a value of 337.28K for the brass-steel couple.

4.2.2. The temperature as a function of displacement

We note that the variation of the temperature is an increasing function with the displacement along the X axis, (392.78K to 393.27K) for a displacement of (0.005 to 0.011), then it decreases from (393.26K to 392.3K) for a displacement of 0.011 to 0, 017mm for the couple copper-steel and it increases between 337.025K to 337.27K, a difference of 0.24K for a displacement of (0.005 to 0.011), then, in observes a small decrease in temperature between (337.27K to 336.82K) for a displacement of (0.011 to 0.017) (Fig.10). The temperature difference between the two couples is 56°C.

4.3. Mechanical behavior

4.3.1. The stress versus the surface

Figure 11 shows the evolution of the stress in steady state at the contact surface of the two sliding couples. The elastic limit between the elastic and plastic domains is not clearly apparent, so a threshold must be set for the elastic limit: we often choose the stress that leads to a certain percentage of deformation, in the case of metals we often hold 0.2% ($\sigma y \approx \sigma y$ 0.2). It can be seen that the maximum value of this stress is 34.667MPa for the pair brass-steel, but 82.1MPa for the couple copper-steel.

4.3.2. The equivalent stress by the Von Mises criterion as a function of displacement

Figure12 gives the equivalent stress in global reference frame as a function of displacement. This figure summarizes the exact point of the pin-disc contact (the maximum stress). In the static case, the maximum shear stress is closer to the contact surface than in the dynamic case. This figure confirms the maximum value of the equivalent stress (82MPa) for the copper-steel couple and 34.66MPa for the brass-steel couple.

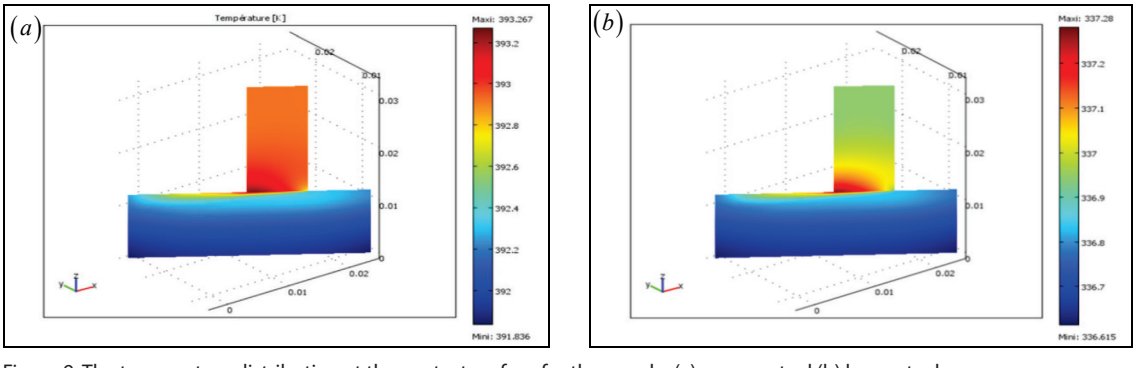

Figure 9: The temperature distribution at the contact surface for the couple: (a) copper-steel.(b) brass-steel.

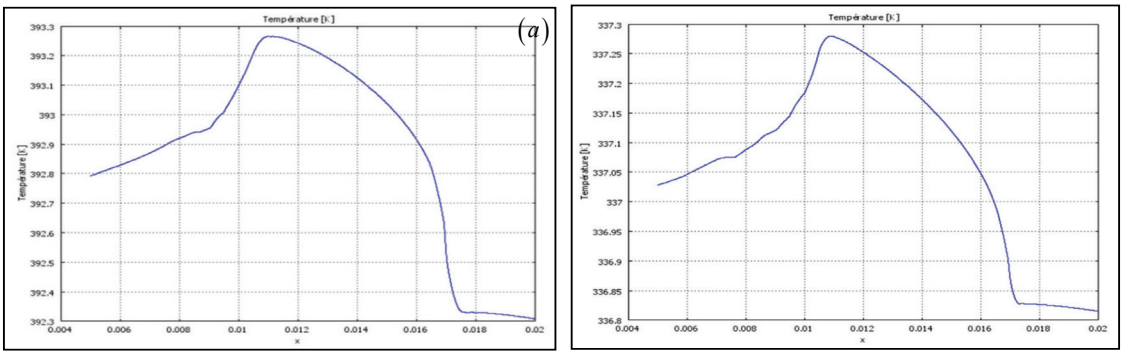

Figure 10: Evolution of the contact temperature versus the displacement in steady state for the couple: (a) copper-steel. (b) brass-steel.

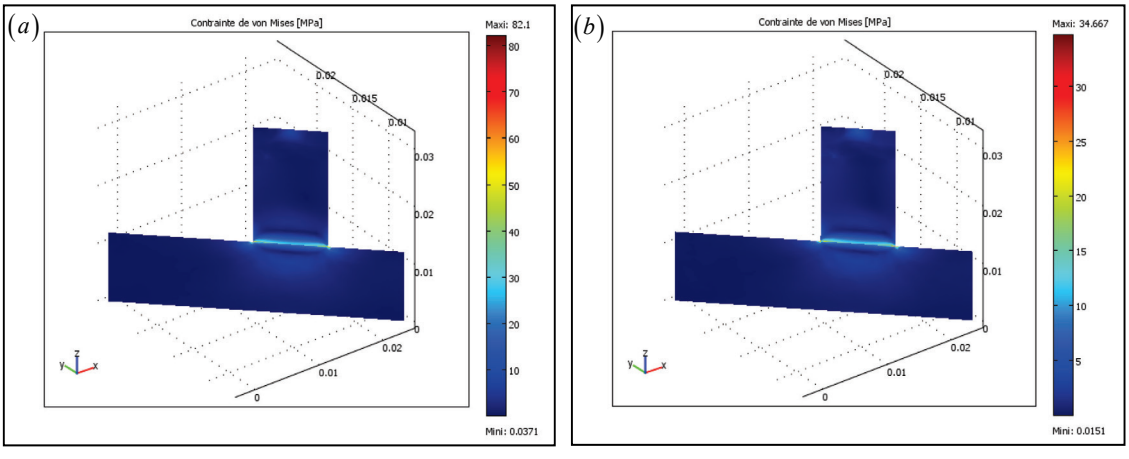

Figure 11: The equivalent stress at the contact surface for the two couples. (a) copper-steel.(b) brass-steel.

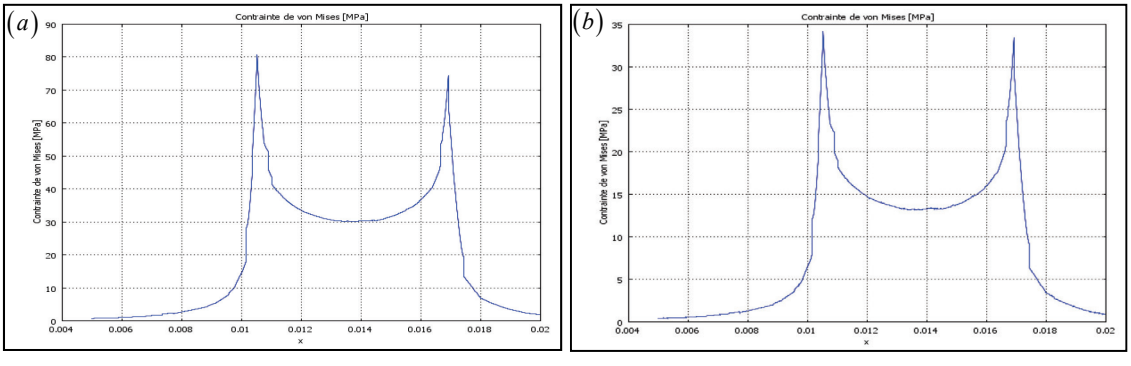

Figure 12: Evolution of the equivalent stress in steady state for the sliding contact: (a) copper-steel. (b) brass-steel.

4.3.3. The contact deformation versus the surface

Figure13 gives the evolution of the maximum elastic deformation (the elastic limit) in steady state at the contact surface for each couple. It can be seen that the closer we get to the contact area, the greater the maximum deformation at the ends of the pin, the higher the values of $1.317.10^{-4}$ for the copper-steel couple and $5.523.10^{-5}$ for the brass-steel couple.

4.3.4. Shear deformation as a function of displacement

Figure14 shows the shear deformation field in the global reference frame as a function of displacement. This curve summarizes the contact points of the real surface. From this curve, we can

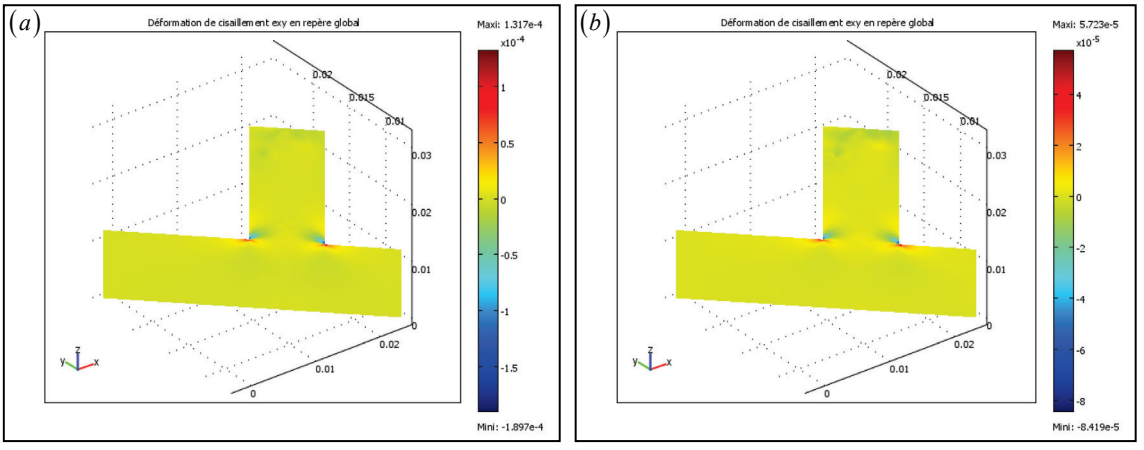

Figure 13: Shear deformation ε_{xy} at a part of the contact surface for the contacts: (a) copper-steel. (b) brass-steel.

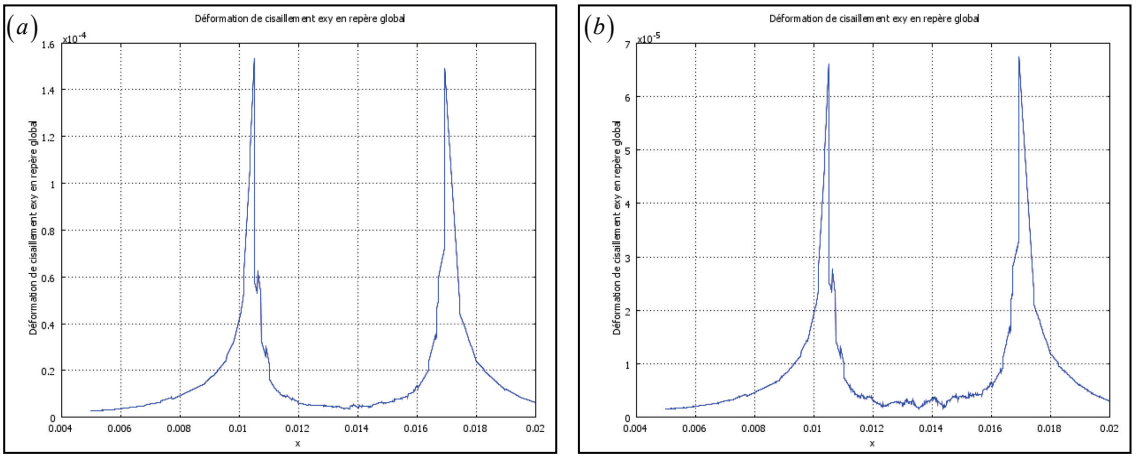

Figure 14: Evolution of the shear strain ε_{xy} for the pairs: (a)copper-steel. (b) brass-steel.

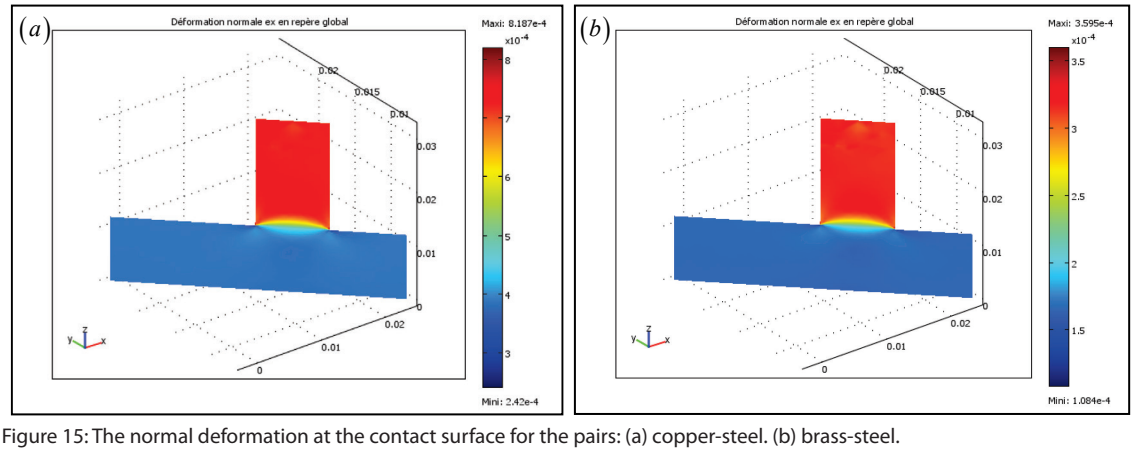

Figure 15: The normal deformation at the contact surface for the pairs: (a) copper-steel. (b) brass-steel.

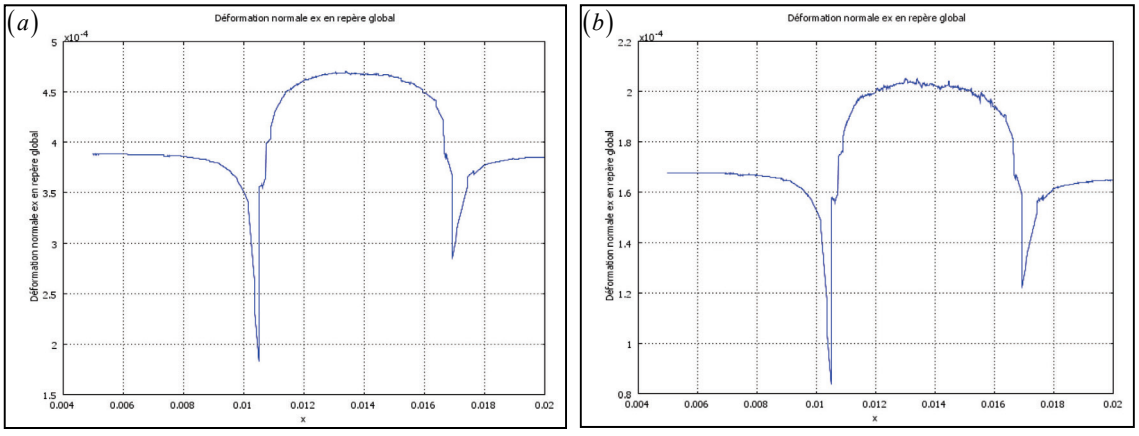

Figure 16: Evolution of the normal deformation in stationary regime for the couples: (a) copper-steel. (b) brass-steel.

see that the maximum deformation points take the values ε=1.5.10^{-4} for X=0.011mm or ε=1.45.10^{-4} for X=0.017 mm in the case of copper-steel pair and the values ε=6.55.10^{-4} for X=0.011mm or ε=6.85.10^{-4} for X=0.017mm in the case of brass-steel pair.

4.3.5. The normal deformation at the contact surface

Figure15 shows the evolution of the normal deformation at the contact surface of the two couples. It can be seen that the closer we get to the contact area, the more the elastic deformation increases to a value of 8.18.10^{-4} for the copper-steel pair and a value of 3.595.10^{-4} for the brass-steel contact, thus a deformation difference of 4.585.10^{-4}.

4.3.6. The normal deformation versus displacement

Figure16 shows the normal deformation of the tribological contact between the pin and the disc, in global reference as a function of displacement. This curve shows the evolution of the normal deformation for the two couples in the displacement interval (X=0.011mm to X=0.017mm) for which ε=2.1.10^{-4} for brass-steel and ε=4.7.10^{-4} for copper-steel.

5. Discussion of the results

The running-in period depends on the test parameters. During this period, the contacts between the elements of the couples are metallic in nature the mutual transfers at the interface are also metallic. There is very little debris in the contact and the coefficient of friction is low μ = 0.26 (copper-steel pair) and μ=0.14 (brass-steel pair) (Fig.4). With time, the debris forms, is torn off and then crushed and plays an abrasive role (Fig.17). As the dynamic contact continues, the adaptation of the surfaces occurs and the mechanism of formation and rupture of the junctions stabilizes by equilibrium of the operating conditions at the interface [7]. In contrast, in the second zone, the friction coefficient is more stable. This stability results from the accommodation of the frictional interface (Fig.4). The asperities are sheared off and there is a significant production of fine particles from both surfaces [7]. The production of particles and the increase in temperature induce a stability of the friction coefficient.

At low loads, the surfaces of the opposing materials touch each other only at the highest asperities. The contact surface increases with the applied load, knowing that under the combined action of this load and the tangential force, the asperities become entangled to form the actual contact surface [8]. After lapping, the surfaces adapt and become smooth, the friction coefficient (μpot) decreases and stabilizes when the operating conditions at the interface become stable (Fig.5).

For low loads, the wear of the pin decreases, due to the limited number of contact points between the surfaces. When the load is increased, the actual contact area and interfacial temperature also increase, which leads to different consequences and in particular facilitates the process of oxide formation and breakdown (Fig.10). On the other hand, the loss of material by adhesion depends on the number of metal junctions and their size. The ambient environment tends to accelerate or slow down the rate depending on whether it favors or hinders the existence of metal-metal junctions and the resulting transfer. Indeed, under low load, the volume worn is considerably proportional to P

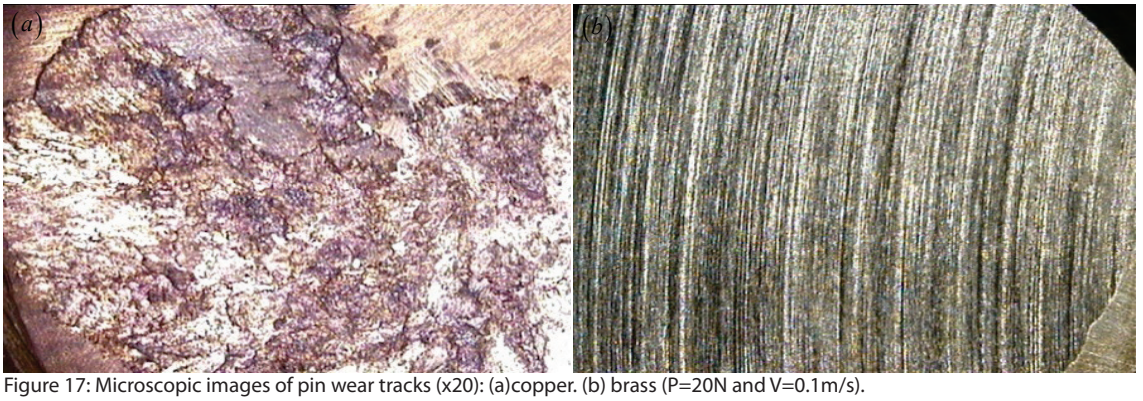

Figure 17: Microscopic images of pin wear tracks (x20): (a)copper. (b) brass (P=20N and V=0.1m/s).

(Fig.8). The increase in the latter is reflected first by an increase in the number of contact points and then by an increase in the size of the junctions. The asperities are plastically deformed (μdef) and thus contribute to a rapid increase in wear (Fig.17).

Moreover, the main effect of the speed is to act on the surface temperature, the maximum temperature reached being that of the most fusible metal (Fig.9). If the low load does not lead to immediate destruction, this increase in surface temperature will have the following effect:

– in the presence of air, most metals oxidize and form oxides with thicknesses ranging from 1 to 10nm [9]. These oxides play a determining role in the tribological behavior, insofar as the operating conditions allow their maintenance or renewal. Indeed, the work of adhesion of oxides is much lower than that of metals, which reduces the term of adhesion of (μad) limiting the appearance of interfacial bonds.

– to create hot spots, which increases the reactivity of the surfaces and the wear products with respect to the surrounding environment and favors all the chemical reactions which can occur during sliding;

– to facilitate (because of the successive heating and cooling) the structural modifications and from a certain level, to trigger mechanisms of diffusion of certain elements. Thus, in the case of steels, we can find martensitic type transformations and certain zones see their carbon content change.

At low speeds (0.1m/s), the exposure time is long and the junctions have enough time to grow and the temperature rise is small. The coefficient of friction is around a moderate value of the order of μ=0.57 for the copper-steel pair and μ=0.3 for the brass-steel pair (Fig.6). In the range of 0.1m/s to 0.2m/s, the wear of the pins is high at the beginning, because of the metal junctions that have time to increase their cross-sectional areas by creep and the actual contact area widens in the direction of movement [10].

The decrease of the friction coefficient and the wear is due, on the one hand, to the decrease of the growth time of the junctions and, on the other hand, to the formation of an oxide layer on the rubbing face of the pin. The latter reduces the friction and protects the surface from damage [11]. For a velocity V higher than 0.2m/s, the rise in temperature at the interface activates oxidation, which increases the growth rate of the oxide layer. The oxide film disintegrates, the friction coefficient stabilizes and wear increases (Fig.6). The transfer of metal onto the disc increases, the friction track shows deformations with furrows ploughed in the direction of movement, characteristic of abrasive wear, especially for the brass-steel pair. However, for the copper-steel couple is mild adhesive one (Fig.17a).

The load and the speed introduce limits, due to deformations in one case, to heating in the other (Figs.13-16). The simultaneous action of P and V can:

– increase the conformity of the surfaces by deformation;

– promote by the rise in temperature the diffusion of elements from one part to another and the formation of compounds at the interface;

– promote surface reactions with the surrounding environment;

– to cause the fusion of the surface layers.

The term μ.P.V expresses the specific power generated in the contact. However, P and V do not have a completely symmetrical action. According to], low velocities place the materials in isothermal conditions from the thermal point of view (thus low contact temperatures) and favor deformations and transformations (Fig.18). High velocities induce adiabatic conditions because the heat does not have time to diffuse, which leads to high surface temperatures and opens the way to thermally induced surface changes (Figs.19-20). Low loads limit mechanical damage, while high pressures

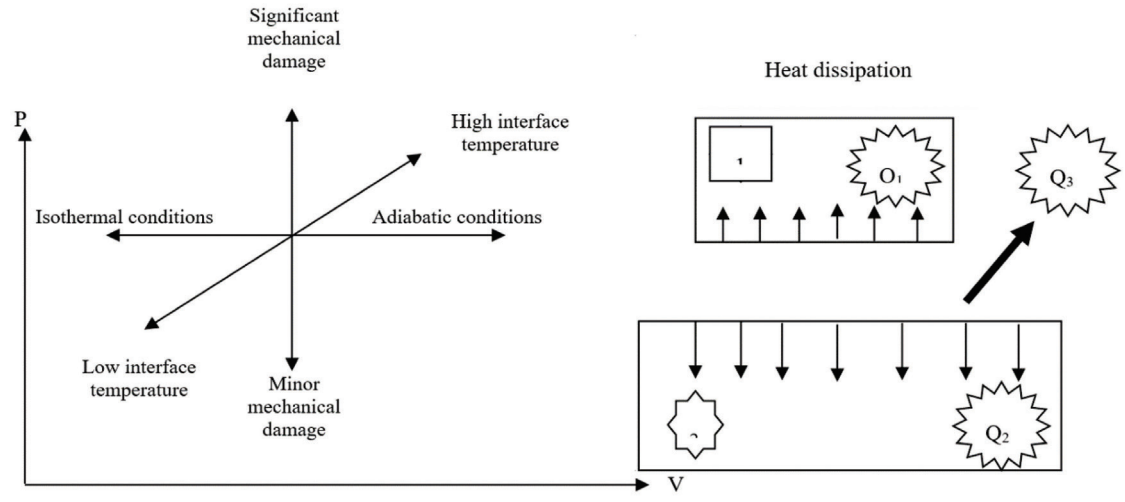

Figure 18: Heat evacuation: diffusion Q1 and Q2 (solids in contact), environment Q3 (convection and radiation).

promote it (Figs.11 and 12). Adhesion between dissimilar metals occurs between 0.35 and 0.5Tf of the more fusible metal [12].

In the common case of triboxidation, [13] showed that several scenarios can occur:

– *oxidation of small metal debris formed during direct contact of the asperities of certain function conditions.*

– *Chemical reactions of the metals constituting the surfaces produce an oxide layer that limits the extent of metal contact, if it is sufficiently adherent and resistant to withstand mechanical stresses (Fig.19 (a)).*

– *Otherwise, this protective layer can fragment and be destroyed by the action of mechanical stresses or by surface fatigue and give rise to debris depending on their nature and properties, the debris also generated can have a beneficial action if they are ductile and lubricating compounds (FeO) or on the contrary, detrimental if they are hard or abrasive (Fe_2O_3) or Fe_3O_4 or for iron (Fig.19 (b)).*

6. Conclusion

This study shows the following:

– *for a normal load of less than 10 N, the coefficient of friction gradually decreases to a value of 0.66 for the copper-steel pair and 0.27 for the brass-steel couple.*

– *for a load greater than 10 N, μ stabilizes at 0.6 for the copper-steel pair and remains constant at around 0.23 for the second pair, since contact surfaces increase as the normal load increases, under the combined action of normal pressure and tangential stress on the one hand. On the other hand, the contact areas touch each other only at the highest asperities, and these asperities interlock to form the actual contact surface.*

– *wear increases with applied load and speed for both sliding couples, and is high for the brass-steel couple. This is due to the greater hardness of copper (HB = 400) than brass (HB = 120).*

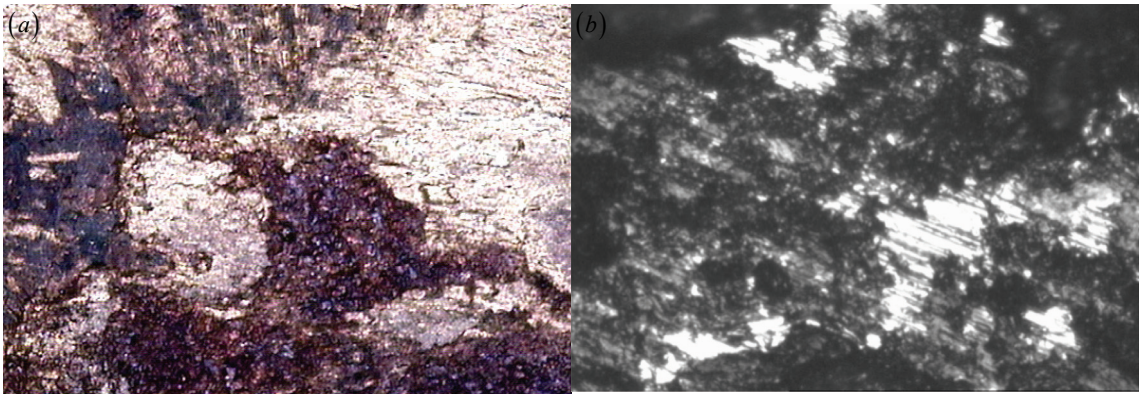

Figure 19: Microscopic images (a): of wear tracks (x20) Copper (P = 20 N and V = 0.5 m/s), (b): of the worn disc face covered with oxide.

– the coefficient of friction is a parameter that has a considerable influence on stress distribution in dynamic contact;

– the contact temperature of the copper-steel pair is higher than that of the brass-steel pair, due to the thermal and physical properties of copper.

– equivalent stress is greater for copper than for brass.

– maximum normal strain is $3.595.10^{-4}$ for brass-steel contact and $8.18.10^{-4}$ for copper-steel contact, therefore a strain difference of $4.585.10^{-4}$.

– the maximum shear strain of the brass-steel pair is low compared with that of the copper-steel couple.

Nomenclature

C_p	**Specific heat at constant pressure, kJ/kg.K**
λ	**Thermal conductivity, kW/m.K**
T	**Temperature, K**
ρ	**Density, kg/m^3**
t	**Time, s**
E	**Elasticity module, kN/m^2**
α	**Coefficient of expansion 1/K**
μ_{pot}	**Potential coefficient of friction**
$\mu_{déf}$	**Deformation coefficient of friction**
μ_{adh}	**Adhesion coefficient of friction**
W	**Wear, g**
P	**Normal load, N**
V	**Speed, m/s**
ε_{xy}	**Shear deformation**
σ_{ij}	**Matrix of the stress, MPa**
h_{air}	**Heat exchange coefficient**
HB	**Brinell hardness**
R_m	**Tear resistant, N/mm^2**

REFERENCES

[1] Boubechou C, Bouchoucha A, Zaidi H (17-19 December 2019). Study of the tribo-thermal behavior of the disc-pin contact. 5th International Conference on Advances in Mechanical Engineering. Istanbul.

[2] Vilarinho C, Davim J. P, and al (2005). Influence of the chemical composition on the machinability of brasses. J. Mater. Process. Technol., Vol. 170, No. 1–2, pp. 441–447, https://www.sciencedirect.com/science/article/pii/S092401360500631X.

[3] F. Schultheiss, D. Johansson, V. Bushlya, J. Zhou, K. Nilsson, and J.-E. Ståhl, (2017). Comparative study on the machinability of lead-free brass, J. Clean. Prod., Vol.149, pp. 366–377. https://portal.research.lu.se/sv/publications/comparative-study-on-the-machinability-of-lead-free-brass.

[4] L. K. Tevfik Küçükömeroğlu, (2014). The friction and wear properties of cuzn39pb3 alloys under atmospheric and vacuum conditions, Wear, Vol. 309, pp. 21–28. https://www.sciencedirect.com/science/article/pii/S0043164813005231

[5] C. Bulthé A. L, Desplanques Y, Degallaix G (2007). Coupling between friction physical mechanisms and transient thermal phenomena involved in pad–disc contact during railway braking", Wear, vol. 263, p. 1230-1242. https://www.researchgate.net/publication/221942863.

[6] Aderghal N (2012). Distribution of heat fluxes generated by mechanical friction and modeling of temperatures at the interface of dynamic Copper-Steel and Copper-Graphite contacts. Doctor of Science in Mechanical Engineering Thesis; Option: Energy. http://archives.umc.edu.dz/handle/123456789/6485.

[7] Bouchoucha A, Chekroud S, Mekroud A (2001). Modeling of heat fluxes generated by sliding friction in a copper-steel contact crossed by an electric current. Sciences and technology. A exact sciences, (15), 63–70. Retrieved from http://revue.umc.edu.dz/index.php/a/article/view/1744.

[8] Boubechou C, Bouchoucha A, Zaidi H (19-21 December 2018). Comparative Analysis of the tribological behavior of copper-steel and brass-steel dynamic contacts. 4th International conference on advances in mechanical engineering, Istanbul. ISBN: 978-605-9546-13-3.

[9] Hor A., Morel F, Lebrun J.L, and Germain G (2013). An experimental investigation of the behaviour of steels over large temperature and strain rate ranges. International Journal of Mechanical Sciences, 67:108 – 122, 2013. ISSN 0020- 7403. doi: https://doi.org/10.1016/j.ijmecsci.01.003.

[10] Okada M, Liou N-S, Prakash V, Miyoshi K. Tribology of high-speed metal-on-metal sliding at near-melt and fully-melt interfacial temperatures. Wear, vo1.249, 672-686,20.

[11] Stalin N, Eytard J.C, Experimental characterization of thermomechanical parameters related to friction, Mechanical & Industrial, vol. 3, 267_270,200.

[12] Mathieu H. J, Bergmann E, Gras R (2003). Analysis and technology of surfaces: thin layers and tribology. PPUR polytechnic presses,

[13] Mouadji. Y (2013). Effect of electric current on the growth mechanism of the oxide layer at the interface of electrodynamic copper-graphite and graphite-graphite contacts. Thesis on science. http://archives.umc.edu.dz/handle/123456789/6485.